

Speed and sensitivity – integration of electrokinetic preconcentration with a leaky waveguide biosensor

Goddard, Nicholas J.; Gupta, Ruchi

DOI:

[10.1016/j.snb.2019.127063](https://doi.org/10.1016/j.snb.2019.127063)

License:

Creative Commons: Attribution-NonCommercial-NoDerivs (CC BY-NC-ND)

Document Version

Peer reviewed version

Citation for published version (Harvard):

Goddard, NJ & Gupta, R 2019, 'Speed and sensitivity – integration of electrokinetic preconcentration with a leaky waveguide biosensor', *Sensors and Actuators B: Chemical*, vol. 301, 127063.

<https://doi.org/10.1016/j.snb.2019.127063>

[Link to publication on Research at Birmingham portal](#)

Publisher Rights Statement:

Goddard, N. & Gupta, R. (2019) Speed and sensitivity - integration of electrokinetic preconcentration with a leaky waveguide biosensor, *Sensors and Actuators B: Chemical*, article no. 127063, <https://doi.org/10.1016/j.snb.2019.127063>

General rights

Unless a licence is specified above, all rights (including copyright and moral rights) in this document are retained by the authors and/or the copyright holders. The express permission of the copyright holder must be obtained for any use of this material other than for purposes permitted by law.

- Users may freely distribute the URL that is used to identify this publication.
- Users may download and/or print one copy of the publication from the University of Birmingham research portal for the purpose of private study or non-commercial research.
- User may use extracts from the document in line with the concept of 'fair dealing' under the Copyright, Designs and Patents Act 1988 (?)
- Users may not further distribute the material nor use it for the purposes of commercial gain.

Where a licence is displayed above, please note the terms and conditions of the licence govern your use of this document.

When citing, please reference the published version.

Take down policy

While the University of Birmingham exercises care and attention in making items available there are rare occasions when an item has been uploaded in error or has been deemed to be commercially or otherwise sensitive.

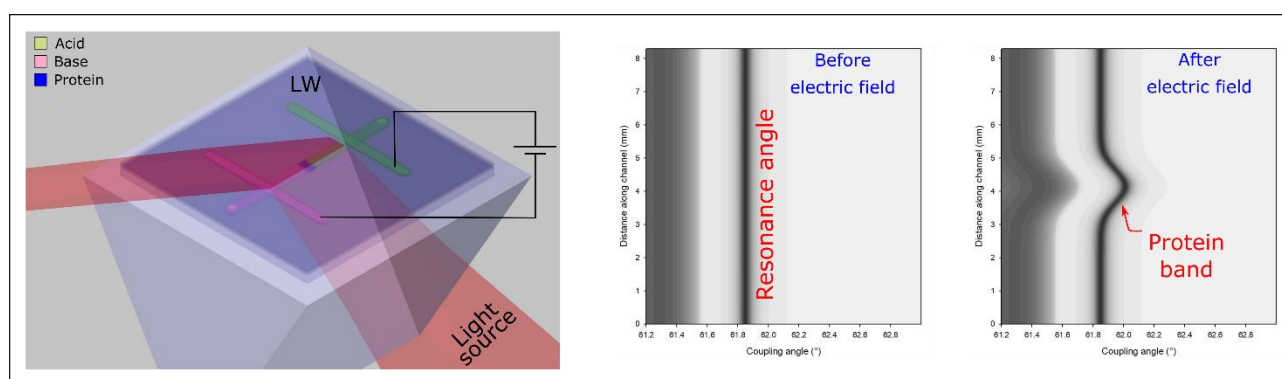
If you believe that this is the case for this document, please contact UBIRA@lists.bham.ac.uk providing details and we will remove access to the work immediately and investigate.

Speed and Sensitivity – Integration of Electrokinetic Preconcentration with a Leaky Waveguide Biosensor

Nicholas J. Goddard, Process Instruments (UK) Ltd, March Street, Burnley, BB12 0BT, UK; Email: nick.goddard@processinstruments.net; Phone: +44 128 242 2835.

Corresponding author: Ruchi Gupta, School of Chemistry, University of Birmingham, Birmingham, B15 2TT, UK; Email: r.gupta@bham.ac.uk; Phone: +44 121 414 6119.

Graphical Abstract:



Abstract: Improving the limit of detection by preconcentration and reducing the response time of optical biosensors are key requirements to enable their use in point of care (PoC) applications. To address these requirements, we have shown that integration of isoelectric focusing (IEF) at a pH step with a leaky waveguide (LW) sensor containing a non-specific affinity ligand (reactive blue 4 dye (RB4)) can reduce the limit of detection of an exemplar protein (bovine serum albumin (BSA)) by a factor of 600 - 930 and reduce the response time to < 60 s. This is 6 - 9 times better preconcentration and up to 16 times faster response time than previous reports. IEF was performed with standard ampholytes and with simple acids and bases forming a pH step. Using ampholytes gave good preconcentration, but was much slower than using a pH step. The LW sensor used a thin agarose hydrogel layer into which RB4 was immobilized. The dye acted both as a non-specific affinity ligand and to visualize the waveguide resonances. This allowed the refractive index of the waveguide to be monitored in real time at any point along the 10 mm separation channel length.

Keywords: Leaky waveguide, electrokinetic preconcentration, response time, limit of detection, point-of-care.

Introduction: Label-free optical biosensors hold promise to allow quantitative measurement of analytes at physiological levels [1] for applications such as point-of-care (PoC) diagnostics [2-4].

An important factor that determines the suitability of a technology for PoC diagnostics is the time required to obtain the results. The acceptable time of response to some extent is determined by the nature of condition being diagnosed, but there has been some consensus on a turnaround of about 15 min [5]. As previously discussed by Eddowes [6], for purely diffusive transport the lower the analyte concentration, the slower the system will be to reach equilibrium. While a response time in the order of minutes or less is obtainable at μM concentrations, inconveniently lengthy response times of hours to days are found at nM or lower concentrations. This in turn reduces the attractiveness of label-free biosensors for PoC diagnosis.

The problem of long response time at low analyte concentrations to some extent has been addressed by performing initial rate instead of equilibrium measurements. The measurement of initial rate is, however, challenging because further improvements in the signal-to-noise ratios are required to obtain the required limit of detection (LOD) for biomarkers. Alternatively, active sample transport to the detection regions has been used by applying electric field [7-9], ultrasound waves [10] and using nanochannels [11, 12]. The use of electric field is popular because it offers benefits such as ease of integration, amenability to automation, speed and portability [13, 14]. Additionally, the approach allows incorporation of sample clean-up along with preconcentration of analytes using discontinuous electrolytes [14-19]. Sample clean-up is particularly relevant for reliable measurement of biomarkers at physiological levels in complex biological samples [20, 21].

A widely used label-free biosensor is surface plasmon resonance (SPR), but the integration of electric field driven sample transport and preconcentration is not feasible because the continuous gold film will short any electric field applied parallel to the sensor surface. Thus, the integration of electrohydrodynamic (EHD) [22] and dielectrophoresis (DEP) [23] has only been demonstrated for SPR gold nanohole arrays. While 100-fold enrichment of a protein (bovine serum albumin, BSA) was demonstrated in 1 min using EHD, it took about 1000 s to preconcentrate the same protein using DEP. The authors stated that the EHD or DEP integrated SPR nanohole array platform required low conductivity solutions limiting their applicability for the analysis of complex biological samples, which are highly conducting because of the presence of salts [24-26]. SPR gold nanohole arrays are typically fabricated using methods such as focused ion beam lithography (FIB) limiting their scope for mass manufacturing. In case of EHD, the need to apply pressure in the range of 4 kPa to drive the analytes through the nanoholes, somewhat reduces the portability of the system by requiring pumps. The instrumentation used to probe and record the output of nanohole array comprised of an inverted epifluorescence microscope and spectrometer/ cooled camera. The high cost of the instrumentation further limits the suitability of the EHD or DEP integrated SPR nanohole arrays for PoC applications.

We address the above limitations by integration of the electrophoresis method isoelectric focusing (IEF) with leaky waveguide (LW) [27-32] detection using a non-specific affinity ligand. By using either ampholytes or simple acids and bases either a pH gradient or step could be formed in the channel. The application of the electric field parallel to the sensor surface distinguishes this

method from others where the field was applied perpendicular to the sensor. In addition, the agarose waveguide only occupied $\sim 2 \mu\text{m}$ of the $275 \mu\text{m}$ depth of the channel, so this was a liquid phase preconcentration, not gel electrophoresis. Previously, a metal-clad LW (MCLW) using a thin titanium layer has been used to apply an electric field perpendicular to the sensor surface to allow bacteria to be rapidly transported to the MCLW for detection [33]. The field could only be applied for a short time to prevent dissolution of the $\sim 10 \text{ nm}$ titanium layer. This is in contrast to the presently described method, where the parallel field could be applied *via* carbon-fibre filled polystyrene electrodes for $>2500 \text{ s}$.

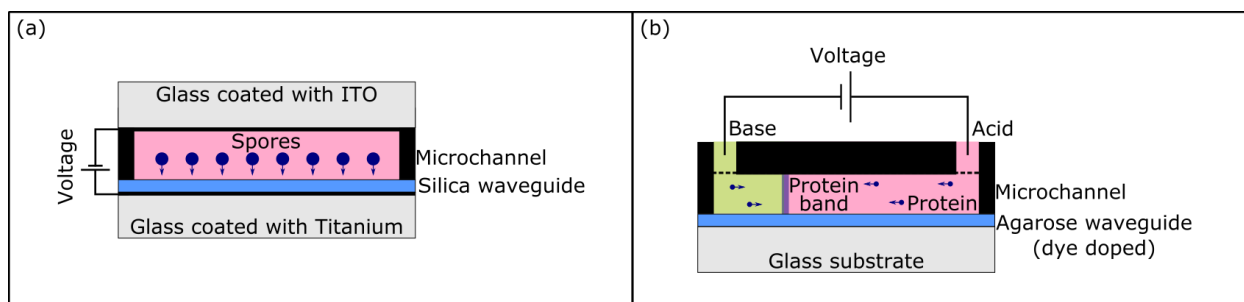


Figure 1: Comparison of (a) previous work using a perpendicular and (b) current work using a parallel electric field to the sensor surface

Proteins such as BSA, hemoglobin (Hb) and myoglobin (Mb) were preconcentrated by three orders of magnitude in times ranging from 60 to 600 s using IEF at a pH step integrated with LW. Proteins were dissolved in 10 mM NaCl to approach the high conductivity of biological samples such as blood and urine. In this work, the LW comprised of a glass substrate coated with a thin porous agarose layer doped with a blue dye, reactive blue 4 (RB4), to permit visualization of the LW resonance and serve as a non-specific affinity ligand. Whole channel imaging in real-time was carried out to track changes in the refractive index (RI) distribution. The changes in the RI of the waveguide are observed as shifts in the resonance angle in the reflectivity curve of the LW. The LW is an all-dielectric structure making its integration with electrophoresis feasible, while still being simple to fabricate by methods such as spin coating and without requiring additional structures/ components. Finally, the instrumentation used to probe and record the output of the LW comprised of affordable and off the shelf components such as a superluminescent diode (SLD) and uncooled CMOS camera. Thus, this work is a significant step towards rapid measurement of analytes at physiological levels for PoC diagnostics.

Experimental:

Chemicals and Materials: 1 mm thick microscope glass slides were purchased from VWR (Leicestershire, UK). Sulphuric acid (H_2SO_4), 25% (v:v) glutaraldehyde (GA), reactive blue 4 (RB4, dye content 35%), phosphoric acid (H_3PO_4), arginine, iminodiacetic acid, Mowiol® (40-88), 1 M hydrochloric acid (HCl), 1 M sodium hydroxide (NaOH), sodium chloride (NaCl), bovine serum albumin (BSA), myoglobin (Mb) and haemoglobin (Hb) were bought from Sigma-Aldrich

(Gillingham, UK). Glycerol and 35 wt% hydrogen peroxide (H_2O_2) were purchased from Fisher (Loughborough, UK). Ultrapure™ LMP agarose was purchased from Life Technologies (Paisley, UK). 40% BioLyte® 3/10 were obtained from Bio-Rad (Hertfordshire, UK). The melting point of the agarose used in this work is 65.5 °C and it sets at temperatures below 25 °C. SnakeSkin™ Dialysis Tubing, 3.5K MWCO membrane was bought from Thermo Fisher Scientific (Altrincham, UK). 275 µm thick double-sided adhesive film (3M 7961MP) was bought from Cadillac Plastics (Swindon, UK). 10 mm thick Perspex was obtained from RS Components (Corby, UK). Crystal clear polystyrene (PS) and 35% carbon fiber-filled high impact PS (CF-PS) granules were purchased from Northern Industrial Plastics (Oldham, UK) and RTP Company (Bolton, UK) respectively.

LW and flow cell Fabrication: Glass slides were cut into ~25.4×25.4 mm squares using a diamond scribe and cleaned in piranha solution (caution – highly corrosive), which was prepared by mixing H_2SO_4 and H_2O_2 in the ratio of 3:1, followed by a thorough wash in de-ionized water. Subsequently, the glass slides were dried overnight at 110 °C in an oven (Mettler, Schwabach, Germany).

2% (w:v) agarose solution was prepared by adding 0.2 g of polymer in 10 ml de-ionized water and heating in a microwave until fully dissolved. The agarose solution was left on a hot plate at 150 °C for 1 h in a closed vial while stirring at 125 rpm. 12.5 µl of 25% (v/v) glutaraldehyde was added and the solution was heated and stirred for another 15 min. Subsequently, the solution was spin coated onto piranha cleaned glass substrates at 3000 rpm for 30 s. RB4 was then immobilized on agarose waveguides by incubating them in a solution containing 20 mg/ml NaCl, 10 mM NaOH and 5 mg/ml RB4 for 1 h followed by a thorough wash in de-ionized water.

The individual layers of the flow cell are shown in Figure 2 (a). The main channel (marked as AA') of width and length of 1.5 mm and 20 mm respectively was laser cut in adhesive 1. Holes of diameter of 1.5 mm were drilled in the membrane and adhesive 2 to serve as inlet and outlet fluidic ports for the main channel. Two slots of width 1.25 mm separated by a centre to centre distance of 11 mm were laser cut in adhesive 2 to form the acidic and basic channels. This resulted in a sample volume between the acidic and basic channels of ~5 µl.

The acidic and basic channels were separated from the main channel *via* a membrane to prevent the proteins in the sample solution in the main channel from diffusing into the acidic/ basic channels, while still allowing the ions to migrate from the acidic/ basic channels to the main channel on applying an electric potential. The top layer of the flow cell was made of Perspex, which was CNC machined to house the injection molded luer connectors. Through holes of 1.25 mm diameter were also drilled in Perspex to access inlet and outlets of the main, acidic and basic channels. The luer connectors fitted in the reservoirs of acid/ basic and main channels were made by injection molding of CF-PS and PS respectively. The luer connectors made of CF-PS also served as electrodes to apply the voltage along the length of the main channel.

Chemicals and Materials: 1 mm thick standard microscope glass slides were purchased from VWR (Leicestershire, UK). Sulphuric acid (H_2SO_4), 25% (v:v) glutaraldehyde (GA), reactive blue 4 (RB4, dye content 35%, acidic form), phosphoric acid (H_3PO_4), arginine, iminodiacetic acid, Mowiol® (40-88), 1 M hydrochloric acid (HCl), 1 M sodium hydroxide (NaOH), sodium chloride (NaCl), bovine serum albumin (BSA), myoglobin (Mb) and haemoglobin (Hb) were bought from Sigma-Aldrich (Gillingham, UK). Glycerol and 35 wt% hydrogen peroxide (H_2O_2) were purchased from Fisher (Loughborough, UK). Ultrapure™ LMP agarose was purchased from Life Technologies (Paisley, UK). 40% BioLyte® 3/10 were obtained from Bio-Rad (Hertfordshire, UK). SnakeSkin™ Dialysis Tubing, 3.5K MWCO membrane was bought from Thermo Fisher Scientific (Altrincham, UK). 275 μm thick double-sided adhesive film (3M 7961MP) was bought from Cadillac Plastics (Swindon, UK). 10 mm thick Perspex was obtained from RS Components (Corby, UK). Crystal polystyrene granules and 35% carbon fibre-filled high impact polystyrene were purchased from Northern Industrial Plastics (Oldham, UK) and RTP Company (Bolton, UK) respectively.

LW and flow cell Fabrication: Glass slides were cut into $\sim 25.4 \times 25.4$ mm squares using a diamond scribe and cleaned in piranha solution (caution – highly corrosive), which was prepared by mixing H_2SO_4 and H_2O_2 in the ratio of 3:1, followed by a thorough wash in de-ionised water. Subsequently, the glass slides were dried overnight at 110 °C in an oven (Mettler, Schwabach, Germany).

2% (w:v) agarose solution was prepared by adding 0.2 g of polymer in 10 ml de-ionised water and heating in a microwave until fully dissolved. The agarose solution was left on a hot plate at 150 °C for 1 h in a closed vial while stirring at 125 rpm. 12.5 μl of 25% (v/v) glutaraldehyde was added and the solution was heated and stirred for another 15 min. Subsequently, the solution was spin coated onto piranha cleaned glass substrates at 3000 rpm for 30 s. RB4 was then immobilised on agarose waveguides by incubating them in a solution containing 20 mg/ml NaCl, 10 mM NaOH and 5 mg/ml RB4 for 1 h followed by a thorough wash in de-ionised water.

The individual layers of the flow cell are shown in Figure 2 (a). The main channel of width and length of 1.5 mm and 20 mm respectively was laser cut in a 275 μm thick double-sided adhesive film (adhesive 1 in Figure 2 (a)). Holes of diameter of 1.5 mm were drilled in the membrane and adhesive film (adhesive 2 in Figure 2 (a)) to serve as inlet and outlet fluidic ports for the main channel. Two slots of width 1.25 mm separated by a centre to centre distance of 11 mm were also laser cut in adhesive 2 to form the acidic and basic channels.

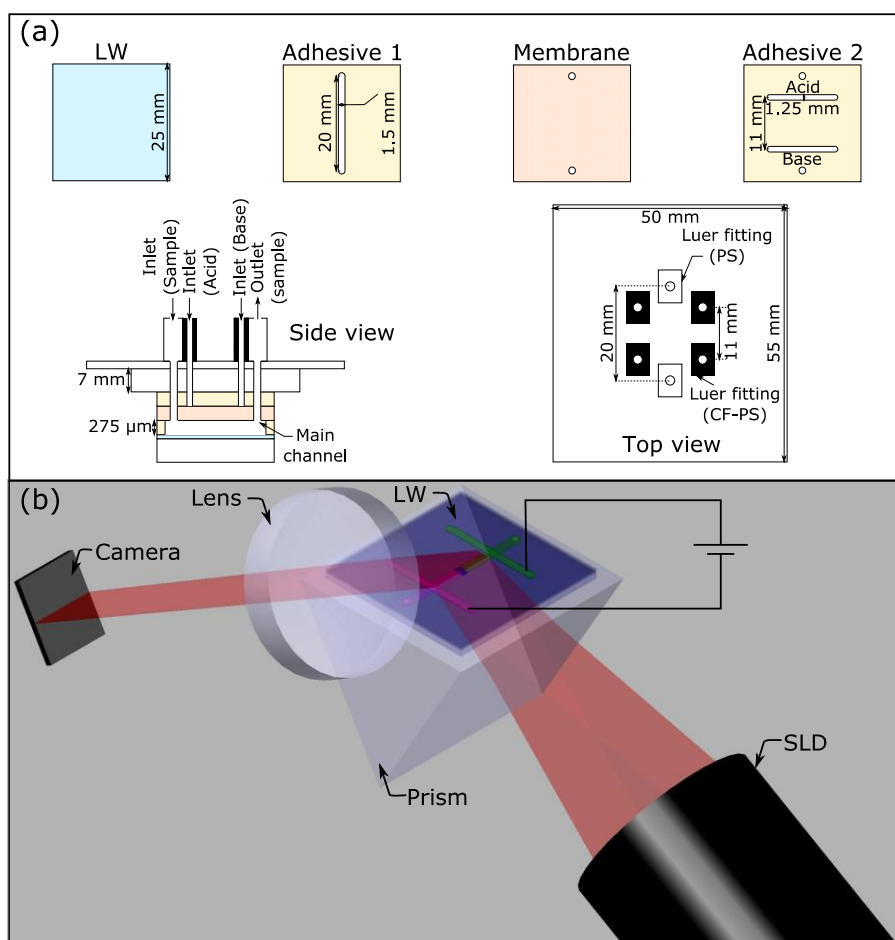


Figure 2: Schematic of the (a) flow cell showing individual layers and cross-sectional view along AA' (where thickness of layers is not to scale), and (b) instrumentation used

Instrumentation: A schematic of the instrumentation is provided in Figure 2 (b). A BK7 equilateral prism (Qioptic Photonics, Denbighshire, UK) was used to couple light in and out of the LW. The prism and LW substrate were optically coupled using a RI matching oil (Type A, Cargille Labs, New Jersey, USA). The light source and the detector were mounted on rails connected to goniometers to allow radial and angular movement respectively. The light source was a 650 nm superluminescent diode (SLD) (EXS210035-02, Exalos AG, Schlieren, Switzerland). The output of the SLD was collimated, expanded to 25 mm diameter and then passed through a 40 mm focal length cylindrical lens to form a wedge beam to probe the LW along the length of the flow channel. The output of the LW was passed through a cylindrical lens and captured on a camera (Pixelink, Ottawa, Canada) with a sensing region of dimensions 10.5 mm by 7.7 mm. The long axis of the camera sensor was aligned parallel to the main channel to allow the whole length of the channel to be imaged.

Solutions were either pumped (Minipuls 3, Gilson, Bedfordshire, UK) or injected manually *via* plastic disposable syringes. Voltage was applied along the length of the main channel using a high voltage power supply (PS350, Stanford Research Systems, California, USA). The RI of

different concentrations of glycerol solutions was measured using an Abbé refractometer with an accuracy of $\pm 1 \times 10^{-4}$.

Methodology: The resonance angle corresponding to the region of the main channel between the acidic and basic channels was imaged on the camera in a single frame. This region was divided into 100 lanes and hence the width of each lane was ~ 0.0975 mm. Out of the 100 lanes, the first 5 lanes and 10 lanes closest to the acidic and basic channels did not contain any useful information. The 85 lanes that were monitored corresponds to a distance of ~ 8.2875 mm. To determine the refractive index sensitivity (RIS) calibration curve, glycerol solutions of different concentrations and hence RI were pumped into the main channel at a flow rate of 0.2 ml/min. The corresponding resonance angle along the length of the main channel was monitored in real-time using a program written in-house using Borland C++ Builder version 6.

To perform isoelectric focusing (IEF), 20 mM H_3PO_4 and 30 mM NaOH (both: with 1% Mowiol[®]) were used as anolyte and catholyte respectively. The anolyte and catholyte also contained 0.5 mM iminodiacetic acid and 5 mM arginine respectively. The main channel was filled with a solution containing 4% ampholyte (pH 3-10), 1 % (w:v) Mowiol[®] and $100 \mu\text{g ml}^{-1}$ BSA. 100 V was applied across the region of the flow channel between acidic and basic channels resulting in an initial current of $\sim 200 \mu\text{A}$ that dropped to $\sim 38 \mu\text{A}$ as the pH gradient was established.

To form a pH step, the acidic and basic channels were filled with 10 mM HCl and 10 mM NaOH respectively. Similarly, the main channel was filled with the sample solution, which comprised of a stock solution of protein diluted in 1 ml of 10 mM NaCl. The typical concentration of the protein in the resulting sample solutions was in the range of 10 to $100 \mu\text{g ml}^{-1}$. Subsequently, 100 V was applied across the region of the flow channel between acidic and basic channels resulting in a typical current of $\sim 130 \mu\text{A}$. The acidic and basic reservoirs were connected to the positive terminal and ground respectively.

Results and Discussion:

Leak waveguide (LWs) are planar structures which in this work was an agarose layer deposited on a glass substrate. Light is partially confined in LWs by total internal reflection (TIR) and Fresnel reflection at the waveguide/ sample and waveguide/ substrate interfaces respectively [30, 31, 34]. The angle at which light is confined in the waveguide, called the resonance angle, may be visualised by incorporation of a dye (in this work, RB4) that absorbs in the wavelength of light used to probe the LW. By doing so, a dip in the reflectivity curve of LW (dark line in Figure 3 (a)) is observed at the resonance angle. The position of the resonance angle is a function of the refractive index of sample on/ in the waveguide and forms the basis of sensing [29, 32, 35].

RIS calibration curve using glycerol: A typical LW output is provided in Figure 3 (a) where the position of the black line corresponds to the resonance angle along the length of the channel. This dark line is observed at the resonance angle because of the presence an absorbing dye, RB4,

immobilized in the agarose waveguide. The position of the resonance angle did not vary much along the length of channel suggesting that the agarose film was of uniform thickness. Additionally, the intensity of the dark line was uniform along the channel indicating that RB4 was homogeneously immobilised in the agarose waveguide.

To determine if the LW was responding equally along the length of the channels, a calibration with glycerol solutions of known RI was performed. A completely uniform waveguide layer would be equally sensitive to RI at any point, but it is unlikely that such a uniform layer is practically realizable. It was important to know the uniformity of the LW, to show that there were no regions where protein could not be detected. A contour plot showing the shift in resonance angle for each lane along the length of the channel for different concentrations of glycerol is provided in Figure S1, SI. Figure S1, SI shows that the change in resonance angle of the LW for different concentrations of glycerol solutions was reasonably uniform along the length of the channel. The distortion observed in Figure S1, SI at $t=2200-2700$ s at a distance of ~ 1.8 mm is attributed to introduction of air bubbles in the channel, which might have been introduced while changing 1.5% (v:v) to 2% (v:v) glycerol solution. Subsequently, for each lane, the shift in resonance angle *versus* RI of glycerol solutions was fitted to a straight line where the slope of the line provided the RIS. As shown in Figure 3 (b), the RIS of the lanes along the length of the channel was similar with an average value of 78.48 ± 8.96 ° RIU⁻¹. The correlation between RI and change in resonance angle was significant ($r > 0.9175$ for 4 degrees of freedom at the 99.5% confidence level for a one-tailed test) for all 85 lanes. A one-tailed test was used as we expect a positive correlation between RI and resonance angle. The lower dashed horizontal line in Figure 2 (b) shows the critical value of the correlation coefficient, while the upper dashed line is for a perfect correlation ($r = 1$). The RI resolution for each lane was estimated from three times the noise on the water part of the glycerol calibration divided by the slope of the calibration line and ranged from 4.53×10^{-6} to 1.28×10^{-4} RIU along the length of the channel. Given the RI increment of BSA in water is ~ 0.16 ml g⁻¹, this means that the LOD for BSA with this sensor was between 28 and 800 $\mu\text{g ml}^{-1}$. Since the instrumental noise is not expected to vary along the channel, the source of this variation is likely to be non-uniformities in the agarose film, which were more significant towards the ends of the channel.

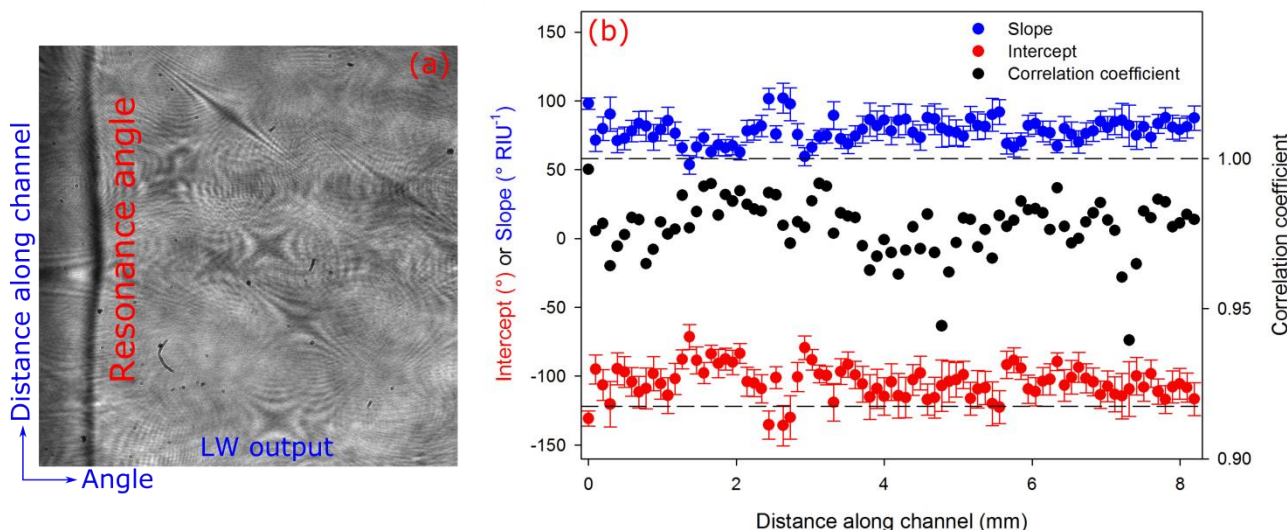


Figure 3: A (a) typical LW output and (b) plot summarising the parameters of the calibration curves of shift in resonance angle versus refractive index of glycerol solutions for all the lanes in the main channel

Analysis of proteins: RB4 was used both to visualise the resonance angle and as a non-specific affinity ligand. The dissociation constant of RB4 with BSA depends on the pH and salt concentration of the solution, but is around 10 μM [36], which is at least 1000 times higher than typical of antibody-antigen interactions. RB4 was used in this study to demonstrate the utility of electrokinetic preconcentration with an immobilised affinity ligand to increase the local concentration of analyte in the waveguide. An initial study was performed using 100 $\mu\text{g ml}^{-1}$ BSA and pH 3-10 ampholyte to implement IEF in the channel with RI sensing using the integrated LW device. Figure 4 shows the resulting changes in resonance angle as a function of time and distance along the channel after application of 100 V at 0 s. As expected, the initial current of 200 μA dropped to 38 μA by 1630 s as the pH gradient became established. The focusing of BSA is clearly visible, but the time taken to form the gradient and for the BSA to migrate to a well-focused zone was about 1600 s. At 2280 s, the preconcentration factor was 520. The position of the BSA zone was not stable, which is most likely a result of electroosmotic flow arising from the negatively charged RB4 used to dope the agarose waveguide. The negative resonance angle shifts visible in Figure 4 as blue areas are probably because of the loss of ampholytes to the anolyte and catholyte reservoirs as the pH gradient was being established. The relatively long time scale to perform preconcentration means that IEF is not likely to be a viable technique for PoC applications.

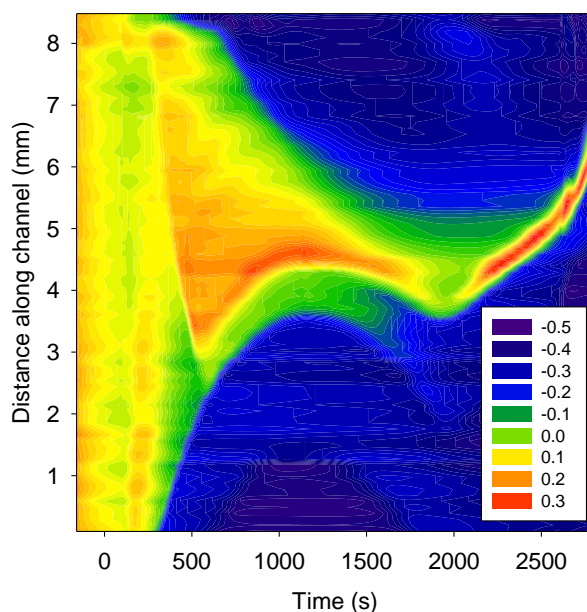


Figure 4: Isoelectric focusing of BSA using pH 3-10 ampholyte where the contours show the change in resonance angle along the length of the channel with time

We subsequently investigated the focusing of BSA using a pH junction, which was formed dynamically on application of a voltage across reservoirs containing 10mM HCl and 10 mM NaOH. On application of the positive potential to the acid and the negative potential to the base reservoir, protons and hydroxide ions are driven into the channel, forming a pH step where the ions meet. Because the electrophoretic mobility of protons is higher than that of hydroxide, the pH step forms closer to the base reservoir. As shown in Figure 5, the resonance angle corresponding to the position 7 to 8 mm away from the acidic reservoir increased within about 60 s after the electric field was applied when the main channel was filled with solution containing the protein. This increase in resonance angle is associated with the preconcentration of BSA and is validated by the absence of such a change in case of the blank, which was 10 mM NaCl without the protein. The blank in Figure 5 shows that the shift in resonance angle as solutions of different pH enter the detection channel is negligible. This in turn suggests that different pH solutions did not cause the agarose waveguide to swell/ contract. The agarose was largely composed of neutral polymer, agarpectin, and hence pH had no measurable effect on the physical dimensions of the waveguide.

The time at which, and location along the channel where, the pH junction was formed and hence the protein was concentrated was determined by a combination of factors such as difference in the electrokinetic mobility of acidic and basic species, pK_a of the dye (in this case, RB4) immobilized in the waveguide to visualize the resonance angle and electroosmotic flow. This position in the channel was consistent for different concentrations of BSA. In comparison to ampholytes, the electrophoretic mobility of anions and cations used to form the pH junction is much higher [37-41]. Thus, the pH junction formation and protein preconcentration was rapidly achieved. For $75 \mu\text{g ml}^{-1}$ BSA, subsequent to when the protein was concentrated to its maximum value, the

width of the protein band began to increase. This band broadening is likely to be because of the high concentration of protein affecting the pH distribution along the channel.

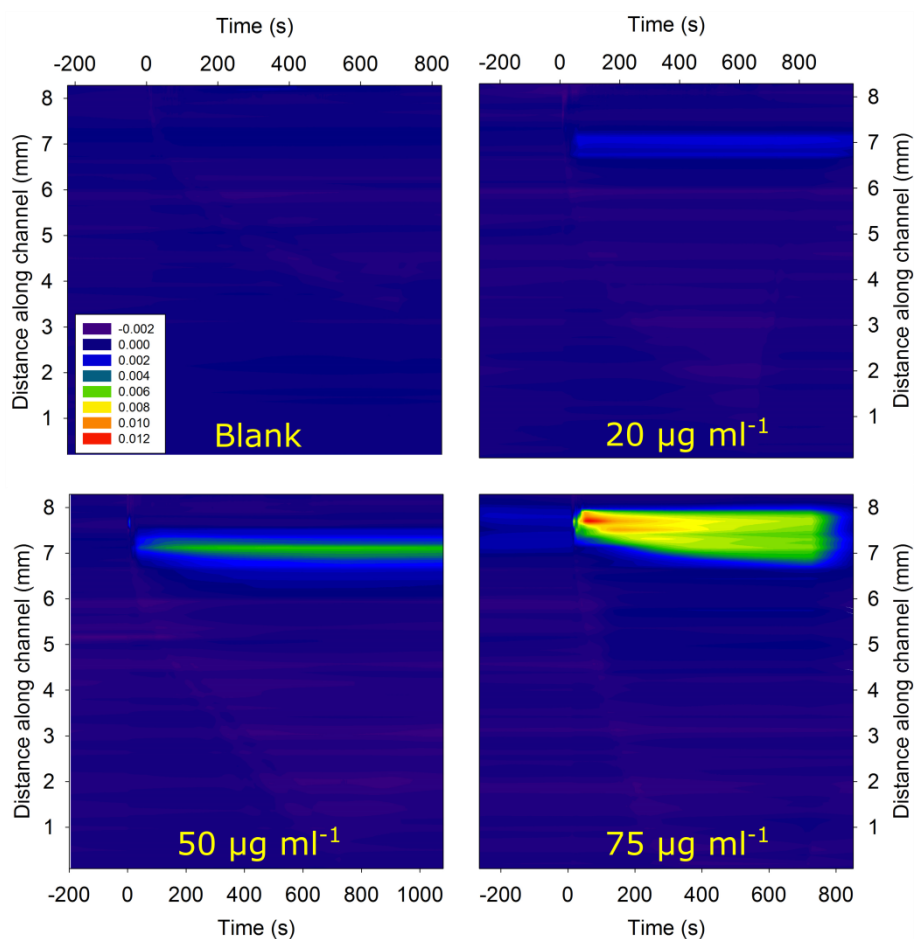


Figure 5: Focusing of BSA using a pH junction where the contours show the change in resonance angle along the length of the channel with time, $t=0$ s represents the time at which voltage was applied and the concentration values are for the initial protein solutions

Figure 6 shows the time course of the preconcentration for BSA concentrations of 20, 50 and 75 $\mu\text{g ml}^{-1}$, where the value plotted at any time point is the maximum resonance angle shift in all the 85 lanes. This clearly shows that for the lower BSA concentrations, the process is rapid, taking about 60 seconds to reach maximum preconcentration. The electrophoretic mobility of BSA varies from $2.8 \times 10^{-8} \text{ m}^2 \text{ V}^{-1} \text{ s}^{-1}$ at pH 3 to $-2.8 \times 10^{-8} \text{ m}^2 \text{ V}^{-1} \text{ s}^{-1}$ at pH 10 [42], which suggests that at 100 V cm^{-1} , it would take about 35 seconds for BSA to travel the length of a 1 cm channel. This is consistent with the observed preconcentration times once diffusion to the sensor surface is taken into account.

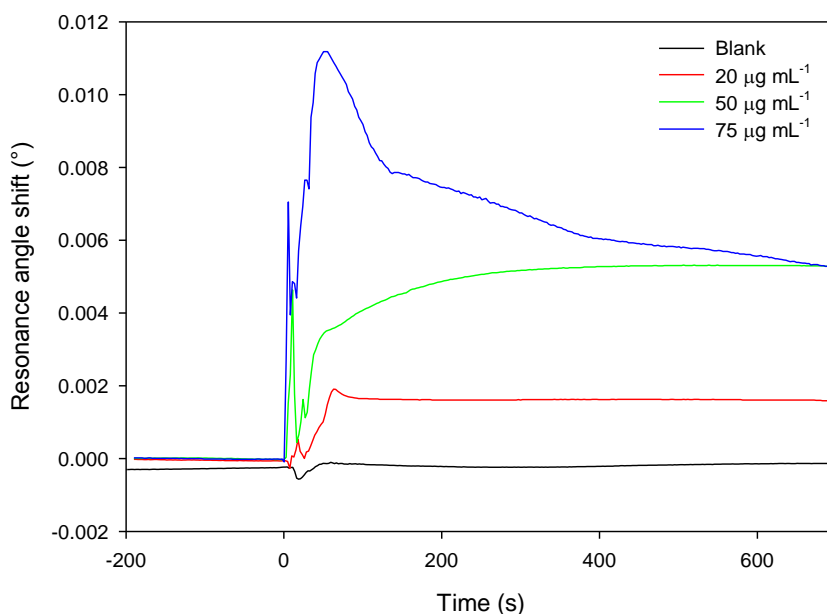


Figure 6: Plot of the time course of the maximum resonance angle shifts for blank and solutions with initial BSA concentrations of 20, 50 and 75 $\mu\text{g ml}^{-1}$ where $t=0$ s is when the electric field was applied

Table 1 summarizes the maximum RI change, maximum concentration and preconcentration factor achieved for each of the initial BSA concentrations. It should be noted that there is no active transport to the LW sensor; the protein is being driven parallel to the sensor surface and has to diffuse to the LW sensor before binding to the RB4, but because electrokinetic transport results in plug flow of ions there is no stagnant layer above the sensor surface. It should be noted that the observed preconcentration factor is a combination of the increased bulk concentration of protein as a result of preconcentration at the pH step and the concomitant increased local concentration in the waveguide as a result of binding to RB4. If the observed preconcentration was purely from electrokinetic preconcentration, the band would have to have a width corresponding to the channel length divided by the preconcentration factor. This would imply a width of protein band between 10 and 16 μm , which is far smaller than that observed. Based on the observed protein band widths, the bulk preconcentration factor was between 25 and 38. These preconcentration factors imply that the limit of detection can be improved by ~ 3 orders of magnitude in a short timescale compatible with PoC applications. This in turn implies that the LOD for BSA after preconcentration using the pH junction integrated with LW was between 0.03 and 1.34 $\mu\text{g ml}^{-1}$ or 0.46 and 20 nM. It should be noted that this LOD has been achieved using a relatively low affinity ligand ($K_D \sim 10 \mu\text{M}$) and thus by using antibodies with dissociation constants $10^3 - 10^4$ times lower [43] potentially we can measure femtomolar to picomolar protein concentrations. More importantly, the integration of pH junction allows us to perform sample clean up and hence potentially measure proteins in complex biological samples.

Initial concentration ($\mu\text{g ml}^{-1}$)	Maximum RI change	Maximum concentration (g ml^{-1})	Bulk preconcentration factor	Total preconcentration factor
20	1.91×10^{-3}	0.0119	37.8	597
50	5.31×10^{-3}	0.0332	27.8	694
75	11.18×10^{-3}	0.0699	25.0	932

Table 1: The maximum RI change, maximum concentration and preconcentration factor achieved for each of the initial BSA concentrations

To demonstrate that the use of pH junction is applicable for concentrating all types of amphoteric molecules, similar studies were also performed for Mb and Hb, and the results are shown in Figure 7. In this case, Hb was pumped into the channel and preconcentrated, then was washed out with 10 mM NaCl solution and replaced with Mb which was also preconcentrated. This showed that there was no carry-over of Hb into the Mb preconcentration. The observed longer preconcentration times were a result of the lower electrophoretic mobilities of Hb and Mb compared to BSA [44]. The position of the two protein bands was different, but the use of whole-channel refractive index imaging allows the protein band to be seen wherever it forms in the channel.

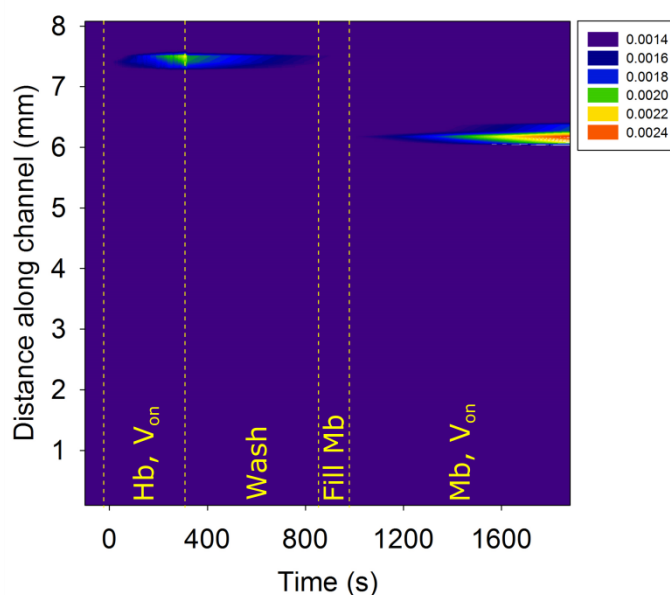


Figure 7: Focusing of Hb and Mb using a pH junction where the contours show the change in resonance angle along the length of the channel where concentration of both Hb and Mb in the initial protein solution was $20 \mu\text{g ml}^{-1}$

4. Conclusions: We have demonstrated the preconcentration of protein analytes by three orders of magnitude within a minute from a $5 \mu\text{l}$ sample volume by integration of electrokinetic preconcentration at a pH step, an electrophoresis method with discontinuous electrolytes,

combined with affinity-based leaky waveguide (LW) whole-channel biosensor. The limit of detection (LOD) of pH step preconcentration integrated with LW was 0.46-20 nM for bovine serum albumin (BSA) using a non-specific affinity ligand with a dissociation constant of $\sim 10 \mu\text{M}$ for the protein. This LOD can be improved by another three to four orders of magnitude with the use of antibody or aptamer based affinity ligands. The pH step integrated LW biosensor is an advance over previously reported work because it offers 6 to 9 times higher preconcentration, up to 16 times faster response time, uses relatively high conductivity sample solutions that better mimic complex biological samples, is easy to fabricate using solution processing methods that are suited for mass manufacturing, and uses affordable instrumentation. Thus, this work is a significant step towards rapid measurement of analytes at physiological levels for point-of-care (PoC) diagnostics.

Conflicts of Interest: There are no conflicts to declare.

Acknowledgements: RG acknowledges the funding support from the Engineering and Physical Sciences Research Council (Grants EP/N02074X/1 and EP/N02074X/2) and Royal Society of Chemistry Tom West Fellowship 2016.

References:

- [1] S. Surinova, R. Schiess, R. Huttenhain, F. Cerciello, B. Wollscheid, R. Aebersold, On the Development of Plasma Protein Biomarkers, *Journal of Proteome Research*, 10 (2011) 5-16.
- [2] F.B. Myers, L.P. Lee, Innovations in optical microfluidic technologies for point-of-care diagnostics, *Lab on a Chip*, 8 (2008) 2015-2031.
- [3] O. Pashchenko, T. Shelby, T. Banerjee, S. Santra, A Comparison of Optical, Electrochemical, Magnetic, and Colorimetric Point-of-Care Biosensors for Infectious Disease Diagnosis, *ACS Infect. Dis.*, 4 (2018) 1162-1178.
- [4] M. Soler, C.S. Huertas, L.M. Lechuga, Label-free plasmonic biosensors for point-of-care diagnostics: a review, *Expert Rev. Mol. Diagn.*, 19 (2019) 71-81.
- [5] A.S. John, C.P. Proice, Existing and Emerging Technologies for Point-of-Care Testing, *Clinical Biochemist Reviews*, 35 (2014) 155-167.
- [6] M.J. Eddowes, Direct Immunochemical Sensing - Basic Chemical Principles and Fundamental Limitations, *Biosensors*, 3 (1987) 1-15.
- [7] R. Vilensky, M. Bercovici, E. Segal, Oxidized Porous Silicon Nanostructures Enabling Electrokinetic Transport for Enhanced DNA Detection, *Advanced Functional Materials*, 25 (2015) 6725-6732.
- [8] M.Y. Chen, M.D. Klunk, V.M. Diep, M.J. Sailor, Electric-Field-Assisted Protein Transport, Capture, and Interferometric Sensing in Carbonized Porous Silicon Films, *Adv. Mater.*, 23 (2011) 4537-4542.

- [9] H.S. Cho, B. Lee, G.L. Liu, A. Agarwal, L.P. Lee, Label-free and Highly Sensitive Biomolecular Detection using SERS and Electrokinetic Preconcentration, *Lab on a Chip*, 9 (2009) 3360-3363.
- [10] M. Zourob, J.J. Hawkes, W.T. Coakley, B.J.T. Brown, P.R. Fielden, M.B. McDonnell, N.J. Goddard, Optical leaky waveguide sensor for detection of bacteria with ultrasound attractor force, *Analytical Chemistry*, 77 (2005) 6163-6168.
- [11] J.H. Lee, Y.-A. Song, J. Han, Multiplexed Proteomic Sample Preconcentration Device Using Surface-patterned Ion-Selective Membrane, *Lab on a Chip*, 8 (2008) 596-601.
- [12] M. Wang, N. Jing, I.H. Chou, G.L. Cote, J. Kameoka, An Optofluidic Device for Surface Enhanced Raman Spectroscopy, *Lab on a Chip*, 7 (2007) 630-632.
- [13] S. Stepanova, V. Kasicka, Analysis of proteins and peptides by electromigration methods in microchips, *J. Sep. Sci.*, 40 (2017) 228-250.
- [14] R. Gupta, S.J. Baldock, P.R. Fielden, J.E. Prest, B.D. Grieve, Isotachophoresis-based sample preparation of cellulases in sugarcane juice using bovine serum albumin as a model protein, *Journal of Chromatography A*, 1217 (2010) 8026-8031.
- [15] C.J. Booker, K.K.C. Yeung, In-Capillary Protein Enrichment and Removal of Nonbuffering Salts Using Capillary Electrophoresis with Discontinuous Buffers, *Analytical Chemistry*, 80 (2008) 8598-8604.
- [16] C.A. Nesbitt, J.T.M. Lo, K.K.C. Yeung, Over 1000-fold protein preconcentration for microliter-volume samples at a pH junction using capillary electrophoresis, *Journal of Chromatography A*, 1073 (2005) 175-180.
- [17] B.C. Giordano, D.S. Burgi, S.J. Hart, A. Terray, On-line sample pre-concentration in microfluidic devices: A review, *Analytica Chimica Acta*, 718 (2012) 11-24.
- [18] Z. Mala, P. Gebauer, P. Bocek, Recent progress in analytical capillary isotachophoresis, *Electrophoresis*, 34 (2013) 19-28.
- [19] G.J. Zhu, L.L. Sun, N.J. Dovichi, Dynamic pH junction preconcentration in capillary electrophoresis-electrospray ionization-mass spectrometry for proteomics analysis, *Analyst*, 141 (2016) 5216-5220.
- [20] J.F. Masson, Surface Plasmon Resonance Clinical Biosensors for Medical Diagnostics, *Acs Sensors*, 2 (2017) 16-30.
- [21] T. Bertok, L. Lorencova, E. Chocholova, E. Jane, A. Vikartovska, P. Kasak, J. Tkac, Electrochemical Impedance Spectroscopy Based Biosensors: Mechanistic Principles, Analytical Examples and Challenges towards Commercialization for Assays of Protein Cancer Biomarkers, *ChemElectroChem*, 6 (2019) 989-1003.
- [22] C. Escobedo, A.G. Brolo, R. Gordon, D. Sinton, Optofluidic Concentration: Plasmonic Nanostructure as Concentrator and Sensor, *Nano Letters*, 12 (2012) 1592-1596.
- [23] A. Barik, L.M. Otto, D. Yoo, J. Jose, T.W. Johnson, S.H. Oh, Dielectrophoresis-Enhanced Plasmonic Sensing with Gold Nanohole Arrays, *Nano Letters*, 14 (2014) 2006-2012.

- [24] F.G. Hirsch, E.C. Texter, L.A. Wood, W.C. Ballard, F.E. Horan, I.S. Wright, The Electrical Conductivity of Blood.1. Relationship to Erythrocyte Concentration, *Blood*, 5 (1950) 1017-1035.
- [25] E.C. Texter, F.G. Hirsch, F.E. Horan, L.A. Wood, W.C. Ballard, I.S. Wright, The Electrical Conductivity of Blood. 2. Relation to Red Cell Count, *Blood*, 5 (1950) 1036-1048.
- [26] L.A. Geddes, L.E. Baker, The Specific Resistance of Biological Material—A Compendium of Data for the Biomedical Engineer and Physiologist, *Medical and biological engineering*, 5 (1967) 271-293.
- [27] R. Gupta, N.J. Goddard, A polymeric waveguide resonant mirror (RM) device for detection in microfluidic flow cells, *Analyst*, 138 (2013) 3209-3215.
- [28] R. Gupta, N.J. Goddard, A novel leaky waveguide grating (LWG) device for evanescent wave broadband absorption spectroscopy in microfluidic flow cells, *Analyst*, 138 (2013) 1803-1811.
- [29] R. Gupta, N.J. Goddard, A proof-of-principle study for performing enzyme bioassays using substrates immobilized in a leaky optical waveguide, *Sensors and Actuators B-Chemical*, 244 (2017) 549-558.
- [30] R. Gupta, N.J. Goddard, Broadband absorption spectroscopy for rapid pH measurement in small volumes using an integrated porous waveguide, *Analyst*, 142 (2017) 169-176.
- [31] R. Gupta, N.J. Goddard, Optical waveguide for common path simultaneous refractive index and broadband absorption measurements in small volumes, *Sensors and Actuators B-Chemical*, 237 (2016) 1066-1075.
- [32] R. Gupta, N. Alamrani, G.M. Greenway, N. Pamme, N.J. Goddard, A Method for Determining Average Iron Content of Ferritin by Measuring its Optical Dispersion, *Analytical Chemistry*, 91 (2019) 7366-7372.
- [33] M. Zourob, S. Mohr, B.J.T. Brown, P.R. Fielden, M.B. McDonnell, N.J. Goddard, An integrated optical leaky waveguide sensor with electrically induced concentration system for the detection of bacteria, *Lab on a Chip*, 5 (2005) 1360-1365.
- [34] R. Gupta, B. Bastani, N.J. Goddard, B. Grieve, Absorption spectroscopy in microfluidic flow cells using a metal clad leaky waveguide device with a porous gel waveguide layer, *Analyst*, 138 (2013) 307-314.
- [35] R. Gupta, N.J. Goddard, A novel optical biosensor with internal referencing, in: 17th Int.national Conference on Miniaturized Systems for Chemistry and Life Sciences, Freiburg, Germany, 2013, pp. 1490-1492.
- [36] J. Liang-Schenkelberg, G. Fieg, T. Waluga, Molecular Insight into Affinity Interaction between Cibacron Blue and Proteins, *Industrial & Engineering Chemistry Research*, 56 (2017) 9691-9697.
- [37] L. Krivankova, F. Foret, P. Gebauer, P. Bocek, Selection of Electrolyte Systems in Isotachopheresis, *Journal of Chromatography*, 390 (1987) 3-16.
- [38] J.C. Reijenga, T. Verheggen, J. Martens, F.M. Everaerts, Buffer capacity, ionic strength and heat dissipation in capillary electrophoresis, *Journal of Chromatography A*, 744 (1996) 147-153.

- [39] J.D. Tissot, P. Schneider, M.A. Duschosal, Two-Dimensional Polyacrylamide Gel Electrophoresis, 1st Edition ed., Academic Press, 2000.
- [40] T. Hirokawa, M. Nishino, Y. Kiso, Isotachophoretic Determination of Mobility and pka by Means of Computer-Simulation.2. Evaluation of mo And pka of 65 Anions, Journal of Chromatography, 252 (1982) 49-65.
- [41] T. Hirokawa, T. Gojo, Y. Kiso, Isotachophoretic Determination of Mobility and pka by Means of Computer-Simulation. 4. Evaluation of mo and pka of 26 Amino-Acids And Assessment of the Separability, Journal of Chromatography, 369 (1986) 59-81.
- [42] B. Jachimska, A. Pajor, Physico-chemical characterization of bovine serum albumin in solution and as deposited on surfaces, Bioelectrochemistry, 87 (2012) 138-146.
- [43] S.D. Jayasena, Aptamers: An emerging class of molecules that rival antibodies in diagnostics, Clinical Chemistry, 45 (1999) 1628-1650.
- [44] U.J. Lewis, B.S. Schweigert, Biochemistry of Myoglobin: iii. Homogeneity Studies with Crystalline Beef Myoglobin, Journal of Biological Chemistry, 214 (1955) 647-655.

Electronic Supplementary Information (ESI)

Speed and Sensitivity – Integration of Electrophoresis with Leaky Waveguide Biosensor

Nicholas J. Goddard, Process Instruments (UK) Ltd, March Street, Burnley, BB12 0BT, UK; Email: nick.goddard@processinstruments.net; Phone: +44 128 242 2835.

Corresponding author: Ruchi Gupta, School of Chemistry, University of Birmingham, Birmingham, B15 2TT, UK; Email: r.gupta@bham.ac.uk; Phone: +44 121 414 6119.

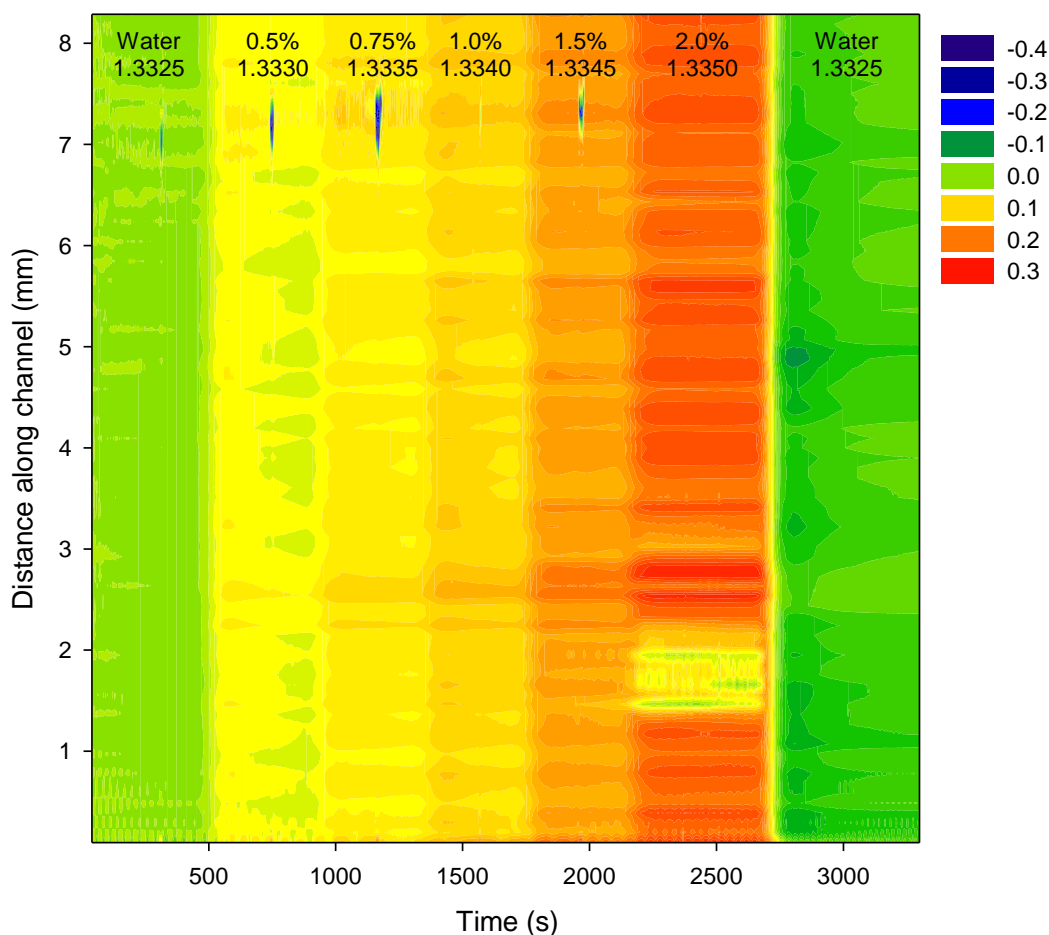


Figure S1: A contour plot of change in resonance angle along the length of the main channel *versus* time as glycerol solutions of different concentrations and hence refractive index were introduced on the LW